System-Wide Case Study Assessment of Transformer Heating Due to Geomagnetic Disturbances

Pooria Dehghanian, *Student Member*, *IEEE*, Komal. S. Shetye, *Senior Member*, *IEEE*,
Katherine R. Davis, *Senior Member*, *IEEE*, and Thomas J. Overbye, *Fellow*, *IEEE*
Department of Electrical and Computer Engineering, Texas A&M University, College Station, Texas, USA
{pooia.dehghanian; shetye; katedavis; overbye}@tamu.edu

***Abstract*—The geomagnetically induced currents (GICs) are a potentially catastrophic threat to large-scale power system operations especially the bulk transformers, possibly leading to severe outages. This paper provides a system-wide transformer temperature analysis due to GIC-induced half-cycle saturation. The derived thermal assessment model identifies the potential overheated transformers in a geomagnetic disturbance (GMD) event and characterizes the relationship between the GIC and the transformer's temperature response. The suggested approach is applied to the 20-bus GIC benchmark test case facing a GMD event, where the time-varying temperature responses are evaluated and numerically analyzed in both normal and hotspot contingency scenarios.**

***Index Terms*— geomagnetic disturbances (GMD); hotspot temperature; transformer; geomagnetic induced current (GIC).**

I. Introduction

GEOMAGNETIC DISTURBANCES (GMD) can have destructive impacts on power system critical infrastructure especially power transformers. Solutions are, hence, required to monitor, control and mitigate such potential threats. Space weather-driven reactions triggered by solar storms (coronal mass ejection) result in space magnetic field variations, which itself induces a geo-electric field at the surface of the earth causing geomagnetically induced currents (GICs) injected into the grounding points of the electric power grid [1].

Power transformers are the most common entry for GICs, resulting in an offset of the ac sinusoidal flux in transformer cores. As a result, when the GICs—characterized by quasi-dc currents—are injected into the power network, transformers may face asymmetric or half-cycle saturation, absorbing higher reactive power, and imposing additional eddy current in various segments of the core, winding, and metallic parts. Such induced overcurrent leads to an intensified temperature rise of transformers' windings and metallic plates [2].

These detrimental effects can appear alone or combined, and may result in system-wide disruptions leading to possible cascades and blackouts. An example of such space-driven natural incidents is a historical GMD event that occurred on March 13, 1989, where people in the northeastern U.S. and especially in Canada experienced a 9-hour blackout—one of the largest outages caused by geomagnetic solar storms in history [3]. Studies of historical GMD events reveal that they have the potential for wide-spread disruptions to power systems depending on the regional latitude and grounding conductivity levels. For instance, Southern Sweden, Hungary, and South Africa experienced a blackout due to geomagnetic storms on October 29, 2003 [4], as a result, a GIC-caused loss of 15 high voltage 400kV transformers was reported in South Africa and thousands of customers lost electricity for hours in Sweden [5].

978-1-5386-9284-4/19/$31.00 ©2019 IEEE

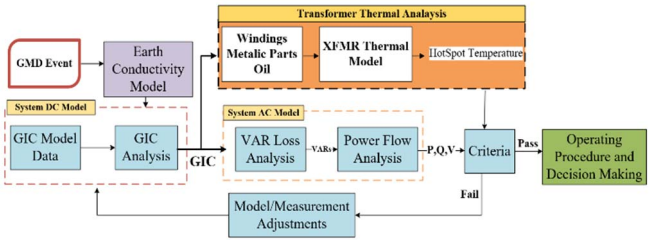

Fig. 1. Overall architecture suggested for thermal analysis of power grid transformers impacted by GICs.

While a GMD is difficult to predict, understanding its formation mechanism and impacts on power grid critical infrastructure can provide insightful information to grid planners and operators. Several efforts in the literature have been reported to monitor [6]-[7], control [8]-[9] and mitigate [10], [11] the impacts of GICs on power networks. Many of the past efforts have focused on GIC monitoring and modeling [12]-[15]. Other aspects of GMD impacts have been also studied: GIC impact on harmonics [16], GIC impact on voltages and generation outputs [17], GIC impact on transformer reactive power losses [18], etc.

Studies have also been conducted to analyze the thermal impacts of GMDs on power transformers. A thermal equivalent circuit of transformers based on a basic heat transfer model is suggested in [19], [20]. Field test research on top oil temperature rise and heating parameter estimation is reported in [21], [22]. A transformer heating assessment is presented in [23] to describe thermal models for hotspot temperature rise in transformers. Thermal impacts of dc currents on power transformers (winding and metallic parts) are investigated in [24]. The impact of GIC on single and three-phase transformers is studied in [25]. A finite element model is utilized in [26] to capture core heating losses. Oil temperature analysis using finite element method is performed in [27] enabling accurate estimation of temperature distribution in transformer windings.

All power transformers across the network may not be equipped with thermal sensors. Among the existing sensors, aging or other equipment issues might make the measurements unavailable or unusable [28].

System-wide thermal assessment of the transformers described in this paper could potentially help grid operators continuously monitor vulnerable equipment. This paper develops, for the first time, a systematic framework to assess the thermal response of transformers during GMD events: (i) analyze the time-varying temperature behavior in normal operating conditions (when all transformers are fully functioning) (ii) contingency scenarios (when a transformer is expected to be thermally damaged), and determine the characteristics of the most thermally vulnerable transformers in the power system. Motivated by the procedure given in [29], Fig.

1 illustrates the suggested architecture for bulk power system analysis impacted by GICs. In our paper, the GIC model is derived based on the North American Electric Reliability Corporation (NERC) benchmark scenario (GMD case 1989) with the peak electric field value of 8 V/km derived from statistical analysis of historical magnetometer data [30]. The corresponding temperature impacts are studied through a thermal analysis model implemented in the 20-bus GIC test case [31].

The rest of the paper is structured as follows. A background on GIC characteristics and its modeling in power systems are introduced in Section II. The derived formulation and transformer thermal model are presented in Section III. Numerical case studies are demonstrated in Section IV, and concluding remarks are mentioned in Section V.

II. GIC Modelling and Characteristics

A. Key Parameters for GIC Characterization

Several parameters are involved in characterizing the GIC flow estimation, including geomagnetic latitude, power grid topology, ground conductivity, and geoelectric field magnitude and orientations [33]. The transmission line length as well as line orientation alignments with corresponding geo-electric fields are considered to be key topological parameters that influence GIC magnitudes in the electric grid. Another critical parameter contributing to GIC magnitudes is the line resistance. GIC magnitudes are more of an issue in low-resistive high-voltage lines than low-voltage lines. Statistics show that when the same level of GICs is injected into different designs of power transformers, the single-phase power transformers have higher GIC-caused saturation vulnerabilities than the three-phase transformers. Three-phase core transformers with three-limb are the least susceptible to GIC-caused saturation [34].

B. GIC Modelling in DC Network Analysis

According to Faraday's law, change of Earth's magnetic field induces geoelectric field above the Earth's surface. If the geoelectric field is assumed to be uniform within the footprint of power system components, it can be represented as $\vec{E}=[E_N, E_E]$ in which E_N and E_E are the Northward and Eastward geoelectric field (V/km) components, respectively. These induced electric fields are the inputs to the GIC model, represented as a dc voltage source connected in series with the ac transmission lines as follows [9], [35]:

$$V(n,m) = E_N\ L_N(n,m) + E_E\ L_E(n,m) \tag{1}$$

where, $L_N(n,m)$ and $L_E(n,m)$ represent the Northward and Eastward distance for a transmission line connecting bus *m* and bus *n*. The dc current injection, I_{dc}, can be assessed using the Norton equivalent model (2) and (3) by taking into account the effective resistance, R_{eff}, such as the line resistance, substation grounding resistance, and transformer winding resistance.

$$I_{dc} = I(n,m) = \frac{V(n,m)}{R_{Eff}} = \sum_{(n,m)} \left(\frac{1}{R_{Eff}} \left(E_N\ L_N(n,m) + E_E\ L_E(n,m) \right) \right) \tag{2}$$

$$\mathbf{V} = \mathbf{G}^{-1}\ \mathbf{I}_{\mathrm{dc}} \tag{3}$$

where, $\mathbf{V} = [V_1, ..., V_n]^T$ is a voltage vector containting dc voltage at any bus and substation neutral, and matrix **G** represents the network conductance matrix, resulted from the bus admittance matrix. The GIC current flow I_{nm} through the transformers located between bus *n* and bus *m* can be calculated as follows:

$$\mathbf{I}_{nm}^{T} = \mathbf{G}_{\mathrm{nm}} . (\mathbf{V}_{\mathrm{n}} - \mathbf{V}_{\mathrm{m}}), \quad \forall n \in \Omega_B, \forall m \in \Omega_S \tag{4}$$

where, Ω_B and Ω_S are the sets of network buses and substations, respectively. $\mathbf{G_{nm}}$ represents the conductance matrix of the transmission line between bus *n* and bus *m*, and it denotes the equivalent conductance with transformer windings. Finally, the linear relationship between the geoelectric field (E) and the dc current injection (2) will yield to transformer GIC:

$$\mathbf{I}_{dc}^{T} = \mathbf{G}_{\mathrm{total}} \sum_{n \in N} \frac{L(n,m)}{R_{Eff}(n,m)} . \mathbf{E} \tag{5}$$

where, $\mathbf{G}_{\mathrm{total}}$ is all the dc conductance (substations, transmission lines, and transformer) quantities.

C. Calculation of Effective GIC on Transformers

The effective GIC is used to measure the impact of the GIC on power transformers. The effective GIC for a wye grounded-delta transformer is equal to the GIC current flow through wye winding. However, in autotransformers and wye grounded-wye transformers both low and high side of the transformer pass the GIC. In this case, the transformer turn ratio should be considered to determine the reflection of the overall impact of dc current on both winding sides. Per phase effective GIC can be calculated using (6):

$$I_{effective}^{GIC} = \frac{\alpha I_H + I_L}{\alpha} = I_H + (\frac{I_N}{3} - I_H)\ V_L \big/ V_H \tag{6}$$

where, I_H and I_N are the high-side and neutral dc current, respectively. V_H is the rated voltage (rms) at high-voltage terminal. V_X is the rated voltage (rms) at low-voltage terminal.

III. Transformer Thermal Modelling: Formulations

A. Transformer Thermal Factors

Thermal stress on power transformers during a GMD event should be evaluated carefully due to dynamic observations on the temperature deviations. Continuous track of the transformer temperature rise during emergency scenarios can help identify the potential overheated transformers. There are three main elements that need to be considered for transformer thermal estimation: oil, windings, and metallic parts (tie plates) [36]. Statistics reported by NERC reveal that the tie plate is the most thermally-vulnerable element in transformers. The temperature rise of the tie plate to a given constant dc current is higher than that for windings [30]. Since the oil has a larger thermal time constant (in the order of hours), the oil temperature variation is relatively low. Another factor is the ambient temperature that can vary hourly and have a direct impact on the total temperature rise. To simplify, a constant oil and ambient temperature are assumed in the simulations.

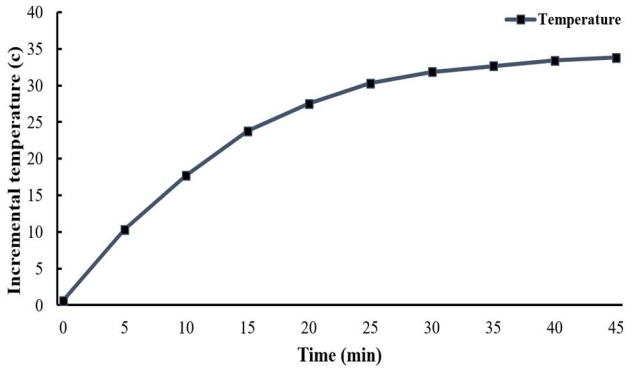

Fig. 2. Metallic hot spot heating curve due to a 16.67 A/phase induced current.

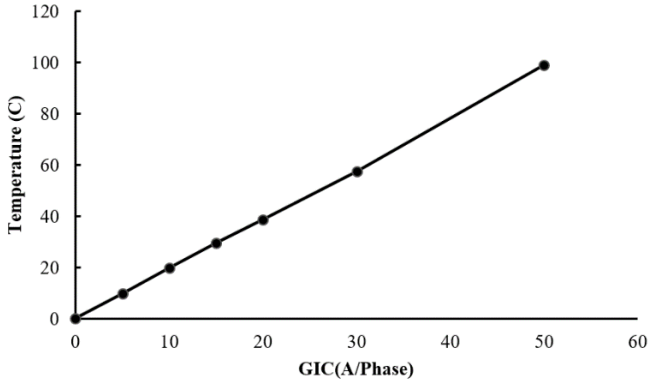

Fig. 3. Asymptotic steady-state hotspot temperature (metallic part) vs. GIC [30].

B. Influence of Temperature rise on Transformer Life-Time

One of the critical parameters which affects a transformer's life is temperature. In fact, the higher temperature rise the less transformer life expectancy. Further, the main cause of transformer failure is insulation damages. Hence, anything that triggers the transformer insulation breakdown (such as moisture, overloading the transformer, poor oil quality, and extreme temperature) reduces transformers life expectancy. However, accurate estimation of loss of transformer insulation life is challenging due to its dependence on time-varying factors such as temperature, moisture, and oxygen content. Thanks to the advanced high-accuracy technologies applied in oil preservation processes, it is assumed that the main factor which contributes to the transformer deterioration and loss of life would be the non-uniform temperature distribution across the winding and metallic parts.

C. Transformer Thermal Model Approximation

Estimation of the transformer thermal response, when the time series injected GIC input data is known, can be accomplished by utilizing either the test measurement data or the manufacture calculations. In so doing, the temperature rise response is approximated based on the measured hotspot thermal response to a given constant current. Fig. 2. illustrates that the temperature rise increases exponentially while a 16.67 A/phase dc step current is injected into the 400 kV transformer' tie-plate [30]. The asymptotic steady-state temperature response to the different levels of current is illustrated in Fig. 3. As can be seen, the final steady-state thermal response to various levels of constant dc currents can be linearly approximated. The approximated step response of the transformer's hotspot rise (see Fig. 2) can be mathematically modeled by a series of exponentials at constant transformer loading as follows:

$$\begin{cases} \Delta\theta(t) = \theta_{ss}(1-\sum_{i=1}^{n} c_i e^{-t/\tau_i}) \\ \theta_{ss} = \Delta\theta_F - \Delta\theta_i \end{cases} \quad (7)$$

$$\begin{cases} \lim_{t\to\infty} \Delta\theta(t) = \theta_{ss} \\ \Delta\theta(t) = 0 \qquad \forall t < 0 \end{cases} \quad (8)$$

where, parameter τ denotes the thermal time constant (here for tie plate), θ_{ss} is the steady state temperature θ_i and θ_F are the initial and final temperature, respectively, c_i is the coefficient of the exponential thermal function, and (8) represents the boundary of the thermal model. Since the steady-state temperature to a given constant current is time-invariant, the heating model is defined as a linear time invariant (LTI) system. The impulse response of the system can be calculated by derivation of the step response as follows:

$$\Delta\theta_h(t) = \sum_{i=1}^{n} \frac{\theta_{ss} c_i}{\tau_i} e^{-\frac{t}{\tau_i}} = h(t) \quad (9)$$

Having derived the thermal impulse response, one can obtain the output (i.e., the temperature in this case) to any given input [i.e. GIC(t)] using a convolution function as follows:

$$\Delta\theta_{HS}(t) = GIC(t) * h(t) \quad (10)$$

The above heating model can be utilized to predict the temperature rise of both windings and metallic part of the transformer [20]. Due to the limited access of the measured GIC-temperature data, the assumption made in modeling and simulations here is that all transformers have the same design characteristics (equal time constant) and follow the above heating curve patterns. The only parameter that should be carefully selected is the time constant since different time constant yields various temperature responses. The model can be generalized if the user-defined time constant is calculated accurately based on the measured test cases. The final hotspot temperature rise can be estimated by adding the oil temperature rise and the ambient temperature to the hotspot temperature model. The oil viscosity changes and this variation with temperature loss may need to be considered for a more accurate oil temperature assessment.

$$\theta_{Final}(t) = \theta_{HS} + \theta_{oil} + \theta_{Ambient} \quad (11)$$

According to the IEEE-C57-12, 2015 [37], particular attention must be paid to long-time transformer operation at rated load above the temperature 110 ˚C. The average and maximum winding threshold on temperature rise above the ambient temperature should not exceed 65 ˚C and 80 ˚C, respectively. Moreover, the transformer hotspot temperature threshold for a short period of time and under full load condition is ~200 ˚C (including oil and ambient temperature). The metallic parts of the transformer in contact with the insulation shall not attain a temperature rise higher than winding hotspot temperature rise at maximum rated load [37].

IV. CASE STUDIES AND NUMERICAL SIMULATIONS

The proposed approach is tested through the 20-bus GIC test case. The algorithms are developed in MATLAB environment and case studies are simulated in PowerWorld (PW) Simulator tool. The benchmark time series electric field derived from a recorded GMD event on March 13, 1989, has been utilized as the input to the developed GIC modeling toolset.

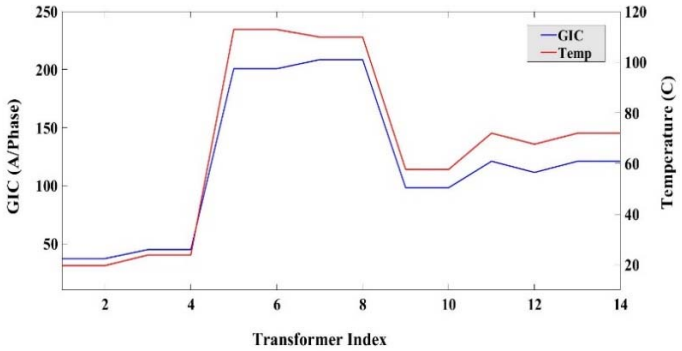

Fig.4 The max. GIC and its corresponding max. temperature rise at all the transformers' tie-plate: During normal operating condition scenario (S1).

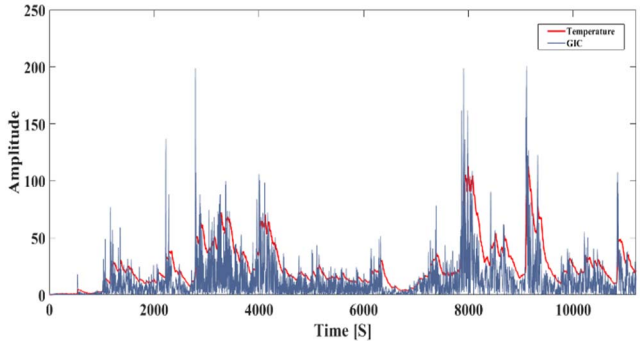

Fig. 5. The dynamic trend of GIC-caused temperature rise over time at the most thermally susceptible transformer tie-plate (T6): During normal operating condition scenario (S1).

TABLE I
CASE STUDY: GIC AND THERMAL RESPONSE OF THE TIE-PLATES (S1)

#	**Bus** (From-To)	**Nominal kV Rate**	**Max. GIC** (A/Phase)	**Max. Temp. (°C)**	**Average GIC** (A/Phase)
T1	3-4	345/500	37.16	19.68	2.17
T2	3-4	345/500	37.16	19.68	2.17
T3	3-4	345/500	44.92	23.86	2.64
T4	3-4	345/500	44.92	23.86	2.64
T5	20-5	345/500	200.7	112.85	13.12
T6	20-5	345/500	200.7	112.85	13.12
T7	6-7	500/22	208.47	109.86	12.08
T8	6-8	500/22	208.47	109.86	12.08
T9	12-13	500/22	98.20	57.62	5.92
T10	12-14	500/22	98.20	57.62	5.92
T11	16-15	345/500	111.34	67.59	7.62
T12	16-15	345/500	111.34	67.59	7.62
T13	18-17	22/345	120.97	71.95	8.13
T14	18-17	22/345	120.97	71.95	8.13

The studied time-varying E-field is in the form of a uniform space spectral across the entire network. The E-field time series data is sampled at a 10s time resolution and used to estimate the GIC(t). The maximum E-field value in the benchmark dataset is 8 V/km. The corresponding GIC values assessed through the time series E-field data set—using (1)-(5)—will be applied as the input to the heating model described in Section III. The hotspot time constant is derived from Fig. 2 and is set to 770 s.

Two scenarios are applied in the case study. In so doing, the transformers' thermal behavior is analyzed in (i) normal operating scenario where all network transformers are fully functional, and (ii) a hotspot contingency scenario where one transformer violates its temperature limit and, thus, eliminated from the system. As a result, the impact of transformer thermal violation on other near-bus transformers are analyzed.

- *Scenario 1 (S1): Normal Operating Condition*

The system under study contains a total of 31 transmission lines, 15 transformers (T), and 7 generating units, with the total capacity of 4780.61 MW, serving a total demand of 4700 MW. The time-variant electric field—which consists of 11,200 E-field data points at a sample rate of 10s—is applied to generate a time series of effective GIC(t) injected in each transformer.

Having calculated the effective GICs flowing into all system transformers as the input to the derived thermal model, the transformer thermal behavior can be traced. Table I displays information of transformers and the maximum and average effective GIC injecting into all network transformers. Fig. 4 illustrates the maximum GIC (A/phase) and its corresponding maximum temperature rise at all the transformers' tie-plate. According to (11), if the oil and ambient temperature values are also taken into account, the transformer temperature rise would be even higher. Note that there is a GIC-blocking device located in substation 1 and, thus, no effective GIC flows into that transformer [31]. The rest of the interested transformers for evaluating their thermal behavior are numbered as can be seen in Table I.

Based on the IEEE-C57-12, the average and maximum temperature threshold should not exceed 65 °C and 80 °C, respectively. From the results presented in Table I, one can realize that although the average GIC (t) flowing in each transformer is relatively low, the maximum temperature rise at some transformers exceeds the average thermal threshold (65 °C). Such a response depends on multiple factors: magnitude and the number of frequencies in GIC pulses greater than 75 A/phase and the time they last (ranging between seconds to minuets).

The study results in Table I reveals that the higher voltage transformers may not always experience a higher-level GIC. For instance, take transformer 1 (T1) as an example: T1 with a higher voltage rating is exposed to a lower GIC than the transformer 13 (T13) with a lower voltage rate.

Normally, the higher GIC level results in higher losses and temperature rise. However, as it can be concluded in Table I and Fig. 4, the transformers (T7 and T8) exposed to the highest GIC peak level of 208.47 A/phase do not experience the highest temperature rise. Numerical results show that the transformers connected between bus 20 and bus 5 (T5 and T6) have the highest temperature peak of 112.8 °C (with lower peak GIC level compared to T7 and T8). The dynamic temperature response of T6 which experienced the highest temperature rise vs. the GIC (t) is illustrated in Fig. 5.

Depending on the geographical location of transformers and seasonal weather the average ambient temperature may vary. Liquid-filled transformers come in standard rises of 55 °C and 65 °C. These values are based on a maximum ambient temperature of 40 °C [38]. Noteworthy to mention that the NERC standard states that the vulnerable transformers are among those which experience GICs above 75 A/phase. In our simulation, all the transformers with the temperature peak above the threshold limit are among those exposed to the GICs higher than 75 A/phase at some time points.

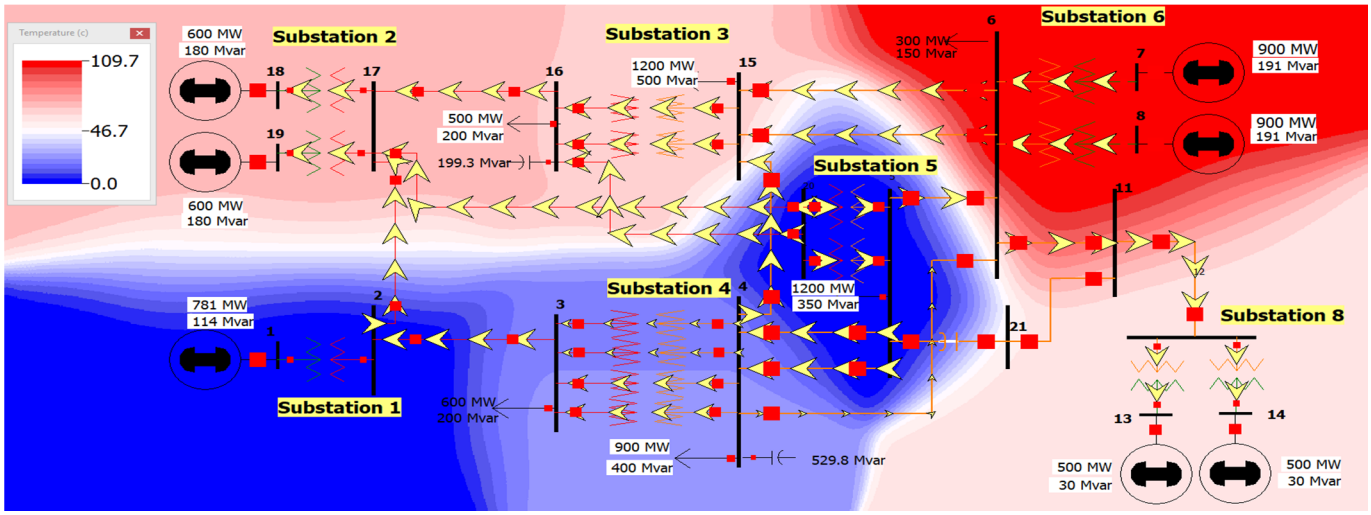

Fig. 6. Transformers' tie-plate temperature rise contour of 20-bus test system: During a contingency operating condition (S2).

Here, for simplicity, we assume an average ambient temperature of ~33 °C and oil temperature of 55 °C. Thus, adding the oil and ambient temperature to the tie-plate temperature detailed in Fig. 4, increases the overall transformer temperature causes the temperature of T5 and T6 exceed the IEEE thermal violation threshold of 200 °C. Thus, in this case, much attention should be paid to monitor the hotspot temperature behavior of these transformers.

- *Scenario 2 (S2): Contingency Operating Condition-Hotspot Temperature Assessment*

According to the IEEE-C57-12, 2015, particular attention must be paid to long-time transformer operation at rated load above the temperature 110 °C. However, the IEEE standard for the short-term hotspot temperature limit is 200 °C. To demonstrate the impacts of the loss of the overheated and/or damaged transformers on the system overall in the worst case scenario, while the ambient and oil temperature are considered to be 33 °C and 55 °C, respectively, a contingency scenario (S2) is analyzed by disconnecting the parallel overheated transformers T5 and T6 located at substation 5. These two transformers experienced the highest tie-plate temperature rise of 112.8 °C during the normal operating scenario (S1) and considering (11) the overall temperature would exceed the IEEE threshold of 200 °C.

Obviously, any modification in the topology of the system changes the electricity flow in the system which results in the variation of temperature response of the transformers across the system. The tie-plate temperature rise contour of the transformers is demonstrated in the one-line diagram of the 20-bus test system presented in Fig. 6. The temperature increases as the contour transits from blue to red. Note that the approximated thermal model of the transformer's tie-plate depends on the GICs input values (10). Although the ambient temperature affects the tie-plate temperature, the simulation results shown in Fig. 6 consider only the role of the GIC changes in the tie-plate temperature rise. Thus, for the substation 1 which is protected by a GIC-blocking device and the post-contingency substation 5 (while transformers are disconnected) the tie-plate's temperature rise contour shows zero value (see Fig. 6). However, the overall transformer temperature value increases when the ambient temperature is considered (11). In this contingency scenario, the maximum temperature rise occurred in T7 and T8. This highlight the facts that, although all other transformers are thermally safe during the normal operating condition, continuous tracking of adjacent transformers to the one faced with the highest GIC is of great necessity in case of contingencies.

V. Conclusions

This paper provides a methodology for a system-wide transformer thermal response assessment in power systems facing a GMD. The derived GIC and thermal assessment models are employed to estimate the dynamic temperature response of the system transformers during normal operating conditions as well as contingency scenarios. The proposed method helps to attain a preliminary system-wide temperature assessment of power transformers to monitor the most thermally-critical elements and prepare for necessary remedial actions.

The GIC-caused temperature impacts on different transformers are studied in the 20-bus test case. A pre and post-contingency thermal assessment is also conducted taking into account the transformer temperature threshold complied with the IEEE standard. Such thermal analyses can help operators monitor and protect transformers and the system to fill in the gaps left by the lack of a sufficient number of sensors, and also as off-line studies for planning and mitigation purposes.

Acknowledgment

This project was funded in part by the National Science foundation (NSF) Award Number: NSF 15-20864.

References

[1] "Geomagnetic disturbances: Their impact on the power grid," in *IEEE Power and Energy Magazine*, vol. 11, no. 4, pp. 71-78, July-Aug. 2013.

[2] S. Arabi, M. M. Komaragiri and M. Z. Tarnawecky, "Effects of geomagnetically-induced currents in power transformers from power systems point of view," in *Canadian Electrical Engineering Journal*, vol. 12, no. 4, pp. 165-170, Oct. 1987.

[3] J. N. Wrubel, "Monitoring for geomagnetic induced current flow effects using existing EMS telemetering," *in Proceedings of the 1991 Power Industry Computer Application Conference*, Baltimore, MD, USA, 1991, pp. 45-49.

[4] D. J. Knipp, "Synthesis of geomagnetically induced currents: Commentary and research," in *Space Weather*, vol. 13, no. 11, pp. 727-729, Nov. 2015.

[5] W. Chandrasena, S. Shelemy and D. Jacobson, "A review of Geomagnetic Disturbance (GMD) effects in Manitoba," *IEEE Power & Energy Society General Meeting*, pp. 1-5, Vancouver, BC, 2013.

[6] P. B. Kotzé, P. J. Cilliers and P. R. Sutcliffe, “The role of SANSA's geomagnetic observation network in space weather monitoring: A review,” in *Space Weather*, vol. 13, no. 10, pp. 656-664, Oct. 2015.

[7] M. Zapella, L. Oliveira, R. Hunt and D. Stewart, "Solving old problems with new technology: How to monitor and measure GIC and OPD currents," *2018 71st Annual Conference for Protective Relay Engineers (CPRE)*, College Station, TX, pp. 1-8, 2018.

[8] C. Basu, et al, “Combining multiple sources of data for situational awareness of geomagnetic disturbances,” *2015 IEEE Power & Energy Society General Meeting*, pp. 1-5, Denver, CO, 2015.

[9] M. Kazerooni, H. Zhu, K. Shetye and T. J. Overbye, “Estimation of geoelectric field for validating geomagnetic disturbance modeling,” *2013 IEEE Power and Energy Conference at Illinois (PECI)*, Champaign, IL, pp. 218-224, 2013.

[10] A. Rezaei-Zare and A. H. Etemadi, “Optimal placement of GIC blocking devices considering equipment thermal limits and power system operation constraints,” in *IEEE Transactions on Power Delivery*, vol. 33, no. 1, pp. 200-208, Feb. 2018.

[11] C. Klauber and H. Zhu, “Power network topology control for mitigating the effects of geomagnetically induced currents,” *50th Asilomar Conference on Signals, Systems and Computers*, Pacific Grove, CA, 2016, pp. 313-317.

[12] K. Shetye and T. Overbye, “Modeling and analysis of GMD effects on power systems: An overview of the impact on large-scale power systems,” in *IEEE Electrification Magazine*, vol. 3, no. 4, pp. 13-21, 2015.

[13] M. D. Butala *et al*., “Modeling geomagnetically induced currents from magnetometer measurements: Spatial scale assessed with reference measurements,” in *Space Weather*, vol. 15, no. 10, pp. 1357-1372, Oct. 2017.

[14] A. B. Birchfield, K. M. Gegner, T. Xu, K. S. Shetye and T. J. Overbye, “Statistical considerations in the creation of realistic synthetic power grids for geomagnetic disturbance studies,” in *IEEE Transactions on Power Systems*, vol. 32, no. 2, pp. 1502-1510, March 2017.

[15] D. H. Boteler, “The evolution of Québec earth models used to model geomagnetically induced currents,” in *IEEE Transactions on Power Delivery*, vol. 30, no. 5, pp. 2171-2178, Oct. 2015.

[16] S. Meliopoulos, J. Xie and G. Cokkinides, “Power system harmonic analysis under geomagnetic disturbances,” *18th International Conference on Harmonics and Quality of Power (ICHQP)*, pp. 1-6, Ljubljana, 2018.

[17] H. Weng, G. Yang, X. Li and X. Lin, “The impact of GIC on system voltage and generator output,” *5th International Conference on Electric Utility Deregulation and Restructuring and Power Technologies (DRPT)*, Changsha, pp. 1736-1739, 2015.

[18] A. Rezaei-Zare, “Reactive power loss versus GIC characteristic of single-phase transformers,” in *IEEE Transactions on Power Delivery*, vol. 30, no. 3, pp. 1639-1640, June 2015.

[19] G. Swift, T. S. Molinski and W. Lehn, “A fundamental approach to transformer thermal modeling. I. Theory and equivalent circuit,” in *IEEE Transactions on Power Delivery*, vol. 16, no. 2, pp. 171-175, Apr 2001.

[20] L. Marti, A. Rezaei-Zare and A. Narang, “Simulation of transformer hotspot heating due to geomagnetically induced currents,” in *IEEE Transactions on Power Delivery*, vol. 28, no. 1, pp. 320-327, Jan. 2013.

[21] G. Swift, T. S. Molinski, R. Bray and R. Menzies, “A fundamental approach to transformer thermal modeling. II. Field verification,” in *IEEE Transactions on Power Delivery*, vol. 16, no. 2, pp. 176-180, Apr 2001.

[22] J. Faiz and M. Soleimani, “Dissolved gas analysis evaluation in electric power transformers using conventional methods: a review,” in *IEEE Transactions on Dielectrics and Electrical Insulation*, vol. 24, no. 2, pp. 1239-1248, April 2017.

[23] “Magnetohydrodynamic electromagnetic pulse assessment of the continental U.S. electric grid: Geomagnetically induced current and transformer thermal analysis,” EPRI Project, 2017.

[24] R. S. Girgis and K. B. Vedante, “Impact of GICs on power transformers: Overheating is not the real issue,” in *IEEE Electrification Magazine*, vol. 3, no. 4, pp. 8-12, Dec. 2015.

[25] X. jing, “Single-phase vs. Three-phase high power high frequency transformers,” M. Sc. Thesis report, Virginia Tech University, [Online]. Available: http://hdl.handle.net/10919/32919.

[26] W. Guan *et al*., “Finite element modeling of heat transfer in a nanofluid filled transformer,” in *IEEE Transactions on Magnetics*, vol. 50, no. 2, pp. 253-256, Feb. 2014.

[27] R. Bouhaddiche, S. Bouazabia and I. Fofana, “Thermal modelling of power transformer,” *IEEE 19th International Conference on Dielectric Liquids (ICDL)*, pp. 1-4, Manchester, 2017.

[28] A. Gholami, A. Srivastava, and S. Pandey, “Data-driven failure diagnosis in transmission protection system with multiple events and data anomalies,” *Journal of Modern Power Systems and Clean Energy*, vol. 7, pp. 767-778, 2019.

[29] “Screening criterion for transformer thermal impact assessment,” NERC project 2013-03.

[30] “Transformer thermal impact assessment white paper,” North American Electric Reliability Corporation (NERC), Project 2013-03

[31] R. Horton, D. Boteler, T. J. Overbye, R. Pirjola and R. C. Dugan, “A test case for the calculation of geomagnetically induced currents,” in IEEE Transactions on Power Delivery, pp. 2368-2373, Oct. 2012.

[32] A. B. Birchfield, T. Xu, K. M. Gegner, K. S. Shetye and T. J. Overbye, "Grid Structural Characteristics as Validation Criteria for Synthetic Networks," in *IEEE Transactions on Power Systems*, vol. 32, no. 4, pp. 3258-3265, July 2017.

[33] K. Zheng, L. Trichtchenko, R. Pirjola and L. G. Liu, “Effects of geophysical parameters on GIC illustrated by benchmark network modeling,” in *IEEE Transactions on Power Delivery*, vol. 28, no. 2, pp. 1183-1191, April 2013.

[34] R. Girgis, K. Vedante and G. Burden, “A process for evaluating the degree of susceptibility of a fleet of power transformers to effects of GIC,” *IEEE PES T&D Conference and Exposition*, pp. 1-5, 2014.

[35] T. J. Overbye, T. R. Hutchins, K. Shetye, J. Weber and S. Dahman, “Integration of geomagnetic disturbance modeling into the power flow: A methodology for large-scale system studies,” *2012 North American Power Symposium (NAPS)*, pp. 1-7, Champaign, IL, 2012.

[36] “IEEE guide for loading mineral-oil-immersed transformers,” in *IEEE Std. C57.91-1995*, 1996.

[37] “IEEE standard for general requirements for liquid-immersed distribution, power, and regulating transformers,” in *IEEE Std. C57.12.00-2015 (Revision of IEEE Std. C57.12.00-2010)*, pp.1-74, 2016.

[38] Copper development association Inc., “Premium-efficiency motors and transformers,”[Online].Available: https://www.copper.org/environment/sustainable-energy/transformers/